

Determination of Surface Tension of Succinonitrile Using a Surface Light Scattering Spectrometer¹

P. Tin,^{2,3} D. Frate,⁴ and H. C. de Groh III⁵

Liquid/vapor interfacial surface tensions of succinonitrile, $\text{NC}(\text{CH}_2)_2\text{CN}$, were measured using noninvasive surface light scattering (SLS) spectroscopy. Succinonitrile (SCN) has been and is being used extensively in materials science and fluid physics research, for example, in several theoretical and numerical studies of dendritic growth. It is an established model material with several essential physical properties accurately known with the exception of the liquid/vapor surface tension, γ_{lv} , at various temperatures. Using the SLS spectrometer, we have experimentally determined the liquid/vapor surface tension of SCN in the temperature range from just above its melting point (58.1°C) to 118°C using this noninvasive method. Previous measurements of SCN surface tension are extremely limited. To the best of our knowledge, this work is the first to measure the surface tension of succinonitrile noninvasively at melt and elevated temperatures. The SLS spectroscopy is relatively new and unique. This technique has several advantages over classical methods: it is noninvasive, has a good accuracy, and can be used to measure the surface tension and viscosity simultaneously, although the viscosity results are not discussed here. The accuracy of values obtained from this technique on some standard liquids is better than 2% for the surface tension and about 10 to 15% for viscosity. Our measurements gave $\gamma_{\text{lv}} = 42.28 - 0.0629T \pm 0.2$ ($\text{mN} \cdot \text{m}^{-1}$), with T in $^\circ\text{C}$, and the viscosity at 60°C is 2.68 ± 0.3 cp for pure SCN.

KEY WORDS: succinonitrile; surface light scattering spectroscopy; surface tension.

¹ Paper presented at the Fourteenth Symposium on Thermophysical Properties, June 25–30, 2000, Boulder, Colorado, U.S.A.

² National Center for Microgravity Research (Fluids and Combustion), NASA Glenn Research Center, Cleveland, Ohio 44135, U.S.A.

³ To whom correspondence should be addressed. E-mail: padetha.tin@grc.nasa.gov

⁴ Microgravity Science Division, NASA Glenn Research Center, Cleveland, Ohio 44135, U.S.A.

⁵ Materials Division, NASA Glenn Research Center, Cleveland, Ohio 44135, U.S.A.

1. INTRODUCTION

Succinonitrile (SCN), a widely used metal analogue, is an established research material, with several key physical properties accurately known [1–3]. Several characteristics make SCN advantageous for use as a model material: it is optically transparent, has a BCC crystal structure, has a low melting point, and has only slightly anisotropic solid/liquid surface tension, γ_{sl} , thus, it solidifies dendritically. In the analysis of phase transformation and flow, including nucleation, dendritic growth, interface stability, Ostwald ripening, and Marangoni flow, SCN has been used extensively as a model material. The surface tension is an important physical parameter in many of these analyses. Surface tension-driven convection (Marangoni convection) is a subject of significant interest from both fundamental and technological points of view. Reliable liquid/vapor surface tension, γ_{lv} , data at various temperatures for SCN and SCN–acetone alloys is needed, for example, for studying the effect of Marangoni convection generated by voids on segregation during the solidification process [4]. The change in γ_{lv} with temperature is the driving force for Marangoni flow. Thus, reliable surface tension values at melt and above the melting point are essential.

Lange's Handbook of Chemistry [5] provides a linear temperature relationship for pure SCN citing data obtained from the capillary rise method which is cited by Jasper [6]. One other data set was found in the literature, from Walden [7]. The technique that Walden used was not described in his paper. Surface tension values given in *Lange's Handbook of Chemistry* [5] are not in good agreement with the values of Walden [7]. Our measurements are the first known noninvasive measurements for SCN at different temperatures. We have demonstrated in this present work that surface tension measurements of succinonitrile at different temperatures can be measured relatively routinely using this noninvasive surface light scattering spectroscopic technique.

2. SURFACE TENSION AND VISCOSITY MEASUREMENTS USING SURFACE LIGHT SCATTERING SPECTROSCOPY

2.1. Surface Light Scattering in Comparison to Standard Surface Tension Measurement Techniques

Techniques commonly used to measure the surface tension of liquid/vapor interfaces can be classified as either equilibrium or dynamic measurements [8]. One of the most common equilibrium techniques is the ring method, or the du Noüy method. This measurement uses a ring of platinum

or platinum–iridium wire to stretch a portion of the liquid surface. The force needed to accomplish this is measured. Another method similar to that above, but still an invasive technique, is the plate method, better known as the Wilhelmy method, which makes use of a platinum rectangular plate. Other equilibrium methods include capillary rise and pendant drop. Techniques for performing dynamic γ_{lv} measurements include the maximum bubble pressure, oscillating jet, and drop volume methods.

These techniques are all invasive methods to measure the required parameters, introducing a mechanical disturbance, which can lead to erroneous results. They all require very precise measurements of parameters that are not easily measured. For an example, in the du Noüy method, the exact circumference of the ring has to be known, and at the same time it has to be dipped parallel to the liquid interface. It also requires a difficult to measure correction factor for the curvature of the liquid interface inside the ring. In the Wilhelmy plate method, the buoyancy correction is required in the case where the bottom of the plate is not tangent to the liquid surface. All in all, an easier-to-use and more accurate test method is desirable. Surface light scattering (SLS) measurements of several standard liquids, such as water, ethanol, and acetone, have shown that the SLS techniques are accurate to better than 2% for γ_{lv} and about 10 to 15% for viscosity [9, 10]. Another advantage of SLS spectroscopy is that it does not introduce any mechanical or thermal disturbance to the liquid or the liquid surface. It also allows for dynamic measurements, unlike many surface tension measurement techniques which have a long response time.

2.2. Determination of Surface Tension and Viscosity Using Surface Light Scattering Spectroscopy

Determination of surface tension and viscosity can be made from the noninvasive measurement of the coherent light scattered from capillary waves generated by thermally excited surface ripples. The theoretical estimate of the amplitude of these surface ripples is of the order of 0.1 Å to a few nanometers. The study and observation of the scattered light from the ripples were first introduced by Katyl and Ingaard [11, 12], and a brief history is given in Langevin's book [13]. This method measures the power spectrum of a narrowly selected group of the surface waves with wavelengths of the order of 0.1 mm, corresponding to frequencies between about 1 and 50 kHz, depending upon the material and temperature. The surface tension and viscosity are then deduced from the acquired autocorrelation function.

In short, the power spectrum, $P(\omega)$, of the ripples for a given \mathbf{k} -vector is contained in the photodetector current measurement and is approximately given by the Lorentzian relation,

$$P(\omega) = a_0 \left[\frac{\Gamma}{\Gamma^2 + (\omega - \omega_0)^2} + \frac{\Gamma}{\Gamma^2 + (\omega + \omega_0)^2} \right] \quad (1)$$

where ω_0 is the center frequency, Γ is the full width at half-height, and a_0 is a scaling constant. The center frequency, ω_0 , and full width at half-height, Γ , are related to the surface tension and kinematic viscosity through the dispersion relation. In the first-order approximation to the solution of the Navier–Stokes equation, these relationships are given by

$$\omega_0(k) = \left(\frac{\gamma}{\rho} \right)^{1/2} |\mathbf{k}|^{3/2} \quad \text{and} \quad \Gamma = 2 |\mathbf{k}|^2 \nu \quad (2)$$

where ρ is the density of the liquid, ν is the kinematic viscosity ($\nu = \nu_d/\rho$, where ν_d is the dynamic viscosity), and \mathbf{k} is the wave vector, where $k = 2\pi/a$ and a is the grating constant. The power spectrum in Eq. (1) is related to the auto correlation function $R(\tau)$ in the time domain by the Wiener–Khinchine theorem and has the form

$$R(\tau) = A + B \cos(\omega_0\tau) \exp(-\Gamma\tau) \quad (3)$$

where A and B are constants and τ is time. Equations (1) and (3) represent measurements which are free from instrumental broadening. Instrumental broadening is common in these types of measurements and is caused by the facts that (a) the laser transverse mode is not completely Gaussian, and (b) the Fourier optics are not exactly aligned. The result is that more than a single scattered light beam (several \mathbf{k} -vectors) combines with the reference beam from the diffraction grating. The effect of instrumental broadening, due to the spread of the \mathbf{k} -vector, is so small that it can be described as a convolution of the Lorentzian spectrum with a Gaussian spectrum assuming that the intensity profile of the laser is generally Gaussian in shape. Equation (3) then becomes

$$R(\tau) = A + B \cos(\omega_0\tau) \exp\{-\Gamma\tau - (\beta\tau)^2/4\} \quad (4)$$

when instrumental broadening is taken into account, where β is the half-width at half-height of the Gaussian spectrum.

The laser heterodyne method (also known as light beating spectroscopy) is used in SLS by introducing a reference signal to beat against the scattered signal. As interest grew in the characterization of thin films

and monolayers, the observation of critical-point phenomena, and the study of biological membranes, this noninvasive laser heterodyne technique progressively improved. Hård et al. [9] developed a SLS system consisting of a grating placed in the optical beam path to create a constant local oscillator. The idea behind this was to project the image of the grating on a liquid–vapor interface and heterodyne beat the scattered signal with the higher-order diffracted beam at the detector plane. This approach provides a constant value local oscillator for heterodyning. It also selects the scattered \mathbf{k} -vector, which is an essential factor in the dispersion relation equation when deducing the surface tension and viscosity. References 13 and 14 give the detailed theory of surface fluctuation spectroscopy using the grating heterodyne detection method. The analysis of the grating heterodyne system by Edwards et al. [14] and Lading et al. [15] provided the corrections required in the data analysis algorithm including the \mathbf{k} -vector broadening effect. Hardware for earlier versions of this heterodyne system was very large and heavy. We have designed, built, and tested a compact, lightweight, and better-performing system using a semiconductor laser and associated optoelectronics for this work.

An alternative way to detect the light scattering from thermal ripplon waves is to split a low-intensity beam from the main incident laser beam and combine it with the scattered signal before it is mixed at the photodetector. Since both the local oscillator light and the scattered light originated from a common laser source whose output is split and recombined downstream, a delay line may be inserted into one of the beam paths to compensate for any path differences. This allows perfect phase matching, mandatory for optical heterodyning when the coherence length of the laser used is short. Mazur et al. [16] used this type of spectrometer to measure surface properties of liquid/vapor interfaces.

Figure 1 shows a schematic diagram of an SLS spectrometer for transmission type geometry mainly useful for optically transparent materials. The spectrometer can also be designed with reflection-type geometry [10]. The functionality of both designs is the same except that transmission is better for transparent materials since forward scattering has a higher intensity and the system is theoretically seven times less vibration-sensitive than the reflective system [17, 18]. Basically, a coherent light source such as a laser illuminates a phase grating, diffracting about 1% of the light power into the first-order beams. The grating is then imaged onto the liquid–vapor interface with a pair of Fourier transform lens. Part of the first-order beam from the grating (only one is needed) directly transmits through the surface as the reference beam. The angle between these beams and the liquid surface selects the wave vector \mathbf{k} of the ripplon wave to be studied. Lenses in the output plane serve as Fraunhofer imaging at the back focal

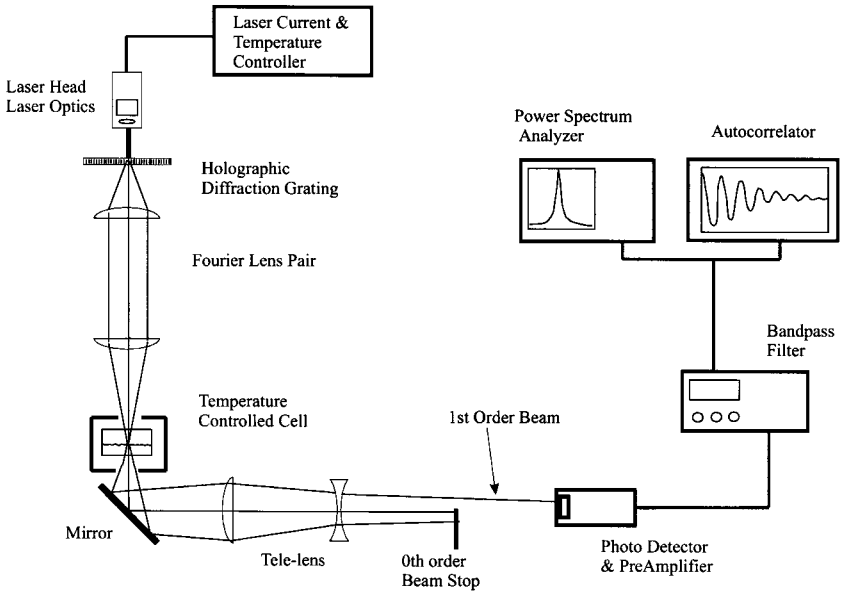


Fig. 1. Surface light scattering spectrometer (transmission type).

plane and also as a tele-lens for angular separation of the first- and zeroth-order beams. The first-order beam is directed onto the photodetector and the photocurrent is amplified, filtered, and finally, processed in an autocorrelator or a spectrum analyzer.

3. EXPERIMENTAL SETUP AND MEASUREMENTS

Since SCN is an optically transparent material, we used the transmission type spectrometer shown in Fig. 1. The SCN was transferred to an optically clear sample container, and the temperature controllers and heaters were added during the experimental setup. A heater at the bottom of the sample container was used to heat the SCN, and a heater at the top of the container was used to prevent SCN condensation on the top surface, which would interfere with the beam. To obtain the sample temperature accurately, a small thermocouple was inserted in the sample. The laser light source used was a gain-guided, broadband, multimode semiconductor laser diode at a wavelength of 670 nm. Mode competition noise and transverse mode beats at the detector plane can degrade the detected current severely, and therefore, the mode structure of the laser in use is of great importance. To suppress the effect of the mode competition noise, a multimode laser

with several longitudinal oscillating modes is preferable to one oscillating with few modes. The reason is that the coherence is reduced with increasing number of longitudinal modes so that the noise spreads over a large bandwidth. For SLS, the theoretical calculation of the required coherence length is about $70 \mu\text{m}$ provided that the surface ripplon amplitude ranges from 0.1 \AA to 10 nm [9]. The diode was powered by the LDC-3742B ILX lightwave laser diode controller. A thermoelectric cooler was set to maintain the laser diode at a constant temperature for power stability during operation. The beam then illuminated a diffraction grating with a grating constant of 250 cm^{-1} developed by Risø National Laboratory. This holographic grating could be adjusted to a diffraction efficiency between 0.5 and 10% of the light into the first-order beams. This made it easier to isolate and strengthen the intensity of a first-order beam at the photodetector downstream.

A single first-order beam from the grating, heterodyned with a scattered light beam, was directed into an Analog Modules, Inc., photodetector, Model 341-4-INV. Signal amplification and filtering were accomplished using an EG&G Princeton Applied Research Model 5113 Pre-Amp filter. The correlator card used was by Brookhaven Instruments Corporation, Model BI 9000. The entire apparatus was mounted on a vibration-isolated optics table.

Figure 2 shows the time correlation function of the SCN liquid/vapor interface measured at 70°C by this technique. The correlation functions were obtained from the Brookhaven Instruments BI 9000 autocorrelator card at different temperatures. The correlation functions were then loaded into an APL 2000 software program that performs a nonlinear least-squares fit on the correlation function, Eq. (4), and calculates the residual. The center frequency, ω_0 , was determined from this fit. The software can also perform the Fourier transform of the correlation function to obtain the power spectrum, which has the shape of a Lorentzian per Eq. (1). The center frequency ω_0 can also be determined in this manner. In both cases, the surface tension is calculated using a more complex version of Eq. (2). A more detailed explanation of this rigorous approach is given by Langevin [13] and Edwards et al. [14]. The full dispersion equations are obtained by solving the linearized Navier–Stokes equation of continuum hydrodynamics with proper boundary conditions accounting for normal and tangential stress at the interface and a mass balance at the surface. This derivation also accounts for an additional correction term for the instrumental broadening effects. System calibration of this apparatus with sets of different grating constants ($250, 500, \text{ and } 700 \text{ cm}^{-1}$) was also performed prior to the measurement of SCN at different temperatures. The surface tension of water, acetone, and toluene were measured and compared to National

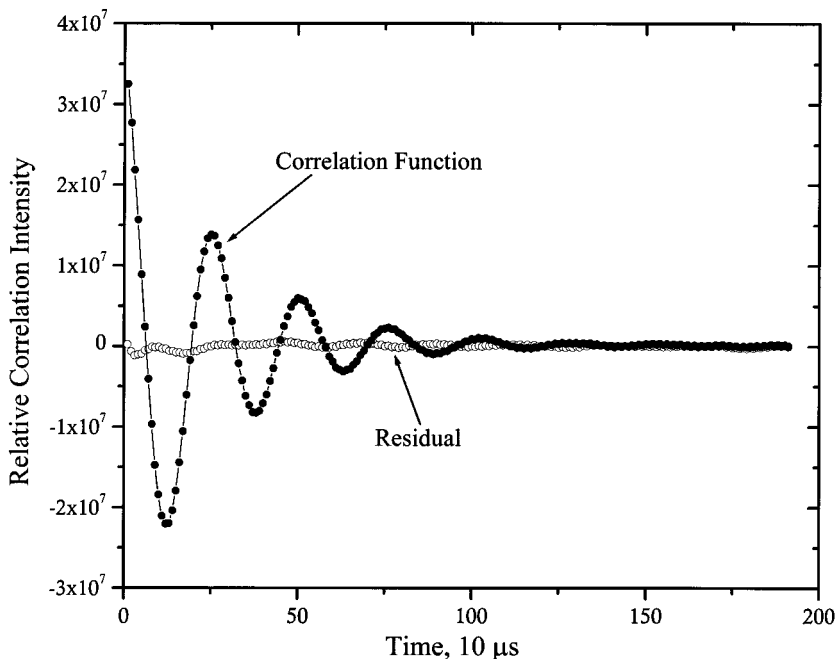


Fig. 2. Typical time correlation function $R(\tau)$ and residual to nonlinear least-squares fit for the SCN liquid/vapor interface using the SLS spectrometer.

Bureau of Standards values, and they agreed to better than 2% for the surface tension and about 10% for the viscosity [9, 10].

Since the SLS method measures thermally driven ripples, an estimate of the temperature rise in the SCN due to absorption of the laser beam was considered. The rate of temperature increase, ΔT , can be expressed as

$$\Delta T = \alpha(\text{laser power/volume})(\text{MW}/(C_p \rho)) \quad (5)$$

For this apparatus, a 100-mW laser beam with a cross section of 7×2.5 mm was imaged on the surface of the liquid. The liquid depth was 5 mm. The molecular weight (MW) of SCN is $80.09 \text{ g} \cdot \text{mol}^{-1}$. The heat capacity (C_p) is $160.18 \text{ J} \cdot \text{mol}^{-1} \cdot \text{K}^{-1}$, and the density (ρ) is $0.988 \text{ g} \cdot \text{cm}^{-3}$ at the melting point. The absorption (α) of SCN was measured experimentally. The power of the laser beam exiting the sample container with the SCN was compared to the power of the laser beam exiting an empty sample container. The result was an absorption of 3% of the laser incident beam by the SCN. Therefore, the calculation of ΔT in Eq. (5) yields $0.02 \text{ K} \cdot \text{s}^{-1}$ for the volume of SCN in the path of the laser beam (0.0875 cm^3). Since measurements

could be taken in 15 s, the temperature change due to the laser beam is negligible. The test configuration introduced a temperature variation of 1°C as a result of the response time of the heaters to the temperature controller.

4. RESULTS AND DISCUSSION

There are limited data in the literature on the surface tension of SCN at various temperatures. A relationship was found in *Lange's Handbook of Chemistry* [5]: $\gamma = a - bT$, where a and b are constants from a least-squares fit and T is the temperature in °C. For SCN, $a = 53.26$ and $b = 0.1079$. The data for this linear fit were cited by Jasper [6], and the technique mentioned was the capillary rise method. The Jasper article incorrectly references Timmerman and Hennaut–Roland [19] as the source of the data, but it is actually a different Timmerman and Hennaut–Roland reference [20]. This source [20] further referenced the data to an untraceable source. The Lange [5] handbook also contained one data point at 80°C and referenced five articles in *Z. Ph. Ch.* published between 1906 and 1911 by Walden. One of these articles contained data for surface tension of SCN at two other temperatures as well [7].

Figure 2 also shows the residual curve of the nonlinear least-squares fit to the time correlation function as calculated by the APL software. It is from this fit that the center frequency, ω_0 , was calculated, and from which the surface tension was determined using Eq. (2) with corrections from Edwards et al. [14]. The SCN density data used in the calculations were obtained from *Beilsteins Handbook of Organic Chemistry* [21]. The least-squares fit to these data yielded the density relationship, $\rho = -0.00075T + 1.0317$, where T is temperature in °C. As stated earlier, the Lorentzian line shape of the power spectrum can also be used to calculate the center frequency and surface tension. As a note, values obtained for the center frequency were of the order of 1 kHz and those for the full width at half-height were a few hundred hertz.

Over a 2-month period, a total of eight data sets was taken. Each data set consisted of measuring the surface tension of SCN at temperatures ranging between 60 and 118°C at 5°C intervals. Two of these data sets had large residuals and were subsequently discarded. Table I shows the surface tension means and standard deviation at each measured temperature. Linear regression fitting and rigorous statistical analysis were performed after pooling the six data sets and the resulting equation was obtained, for T in °C,

$$\text{Surface tension} = 42.28 \text{ (mN} \cdot \text{m}^{-1}) - 0.0629 \text{ (mN} \cdot \text{m}^{-1} \cdot \text{T}^{-1}) T \quad (6)$$

Table I. Mean and Standard Deviation of SCN Surface Tension Experimental Data

Temperature ($^{\circ}\text{C}$)	Surface tension mean ($\text{mN} \cdot \text{m}^{-1}$)	SD, σ
60	37.84	3.059
65	39.09	1.385
70	37.85	2.535
75	38.76	2.322
80	38.15	1.719
85	36.93	3.125
90	37.01	2.211
95	36.23	2.826
100	36.14	2.114
105	36.64	1.864
110	34.45	4.065

Table II lists the surface tension as predicted by Eq. 6 as well as the calculated data from the equation of Lange [5] and the three data points from Walden [7] for comparison. These data are plotted in Fig. 3. The relationship established in Eq. (6) by these experiments yields surface tension data that are about 17% below the Lange relationship [5] and about 9% above the Walden data [7]. Statistics were performed on the regression curve fit of Eq. (6) to bound the confidence level on the fit itself and to confirm the temperature dependence for the surface tension. The result was that there is a 99.95% confidence level that the slope of the regression

Table II. Surface Tension ($\text{mN} \cdot \text{m}^{-1}$) of SCN Measured with the Surface Light Scattering (SLS) Spectrometer as a Function of Temperature Compared to Values from the Literature

Temperature ($^{\circ}\text{C}$)	Data from SLS [Eq. (6)]	Lange prediction [5]	Walden data [7]
60	38.51	46.79	
65	38.19	46.25	
70	37.88	45.71	
75	37.56	45.17	
80	37.25	44.63	34.3
85	36.93	44.09	
90	36.62	43.55	
95	36.30	43.01	
100	35.99	42.47	32.7
110	35.36	41.39	
118	34.86	40.53	31.1

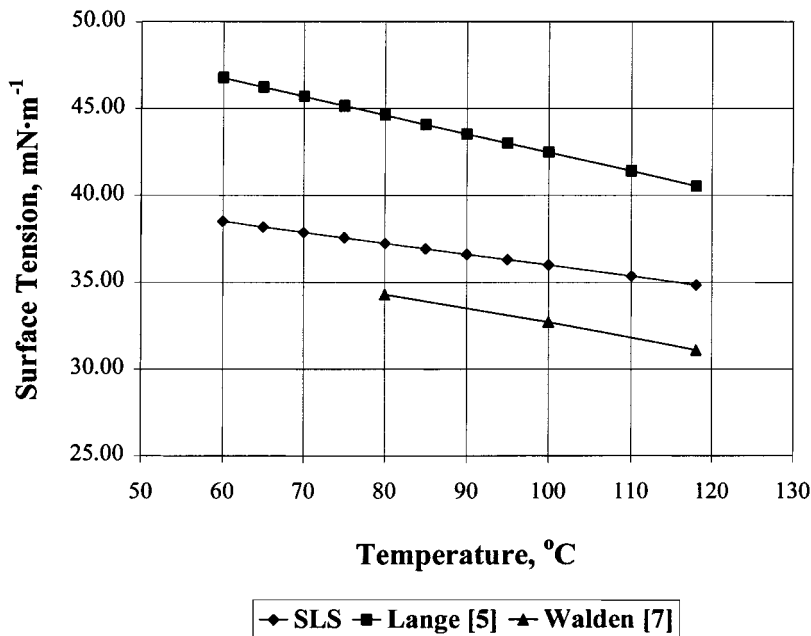


Fig. 3. Surface tension of SCN as a function of temperature.

line is not zero, indicating that the data show that the surface tension is a function of temperature even with some apparent variation in the data.

Some possible sources of error include the lack of tight control on the heaters used. Higher-purity SCN would also improve the measurements. The purity of the SCN was not known exactly. It was most likely no better than 99.9% pure at the time of purchase and may have been even less pure after introduction to the sample container. Impurities have a strong effect on the surface tension and can also interfere with the laser beam corrupting the measurement.

5. CONCLUSIONS

Surface light scattering successfully determined noninvasively the surface tension of succinonitrile in the temperature range from 60 to 110°C. There was some variation in the test data, but much of this variation can be attributed to the control parameters of the experiment. Comparisons to the limited literature database showed that the regression fit of the experimental data falls in between the two data sets found in the literature. Work is in progress for making these measurements with a sample container

temperature controller of better than 0.1 K with higher-purity SCN and with SCN–acetone alloys.

ACKNOWLEDGMENTS

We would like to acknowledge Prof. J. A. Mann, Case Western Reserve University, for theoretical discussions on the surface light scattering techniques and for the implementation and analysis of the APL 2000 surface light scattering software which he developed. Part of the instrumentation work was supported by an Advanced Technology Development project under the sponsorship of the Microgravity Science Division, NASA Glenn Research Center.

REFERENCES

1. M. Kassemi and N. Rashidnia, *Steady and Oscillatory Flows Generated by a Bubble in 1-g and Low-g Environments*, AIAA 97-0924, Reno (1997).
2. B. W. Mangum and S. El-Sabban, NBS Special Publ. 260-101, SRM 1970: Succinonitrile Triple Point Standard—A Temperature Reference Standard Near 58.08 C (1986).
3. M. A. Chopra, M. E. Glicksman, and N. B. Singh, *J. Crystal. Growth* **92**:543 (1988).
4. M. Kassemi, M. Kaforey, and D. Matthiesen, *Effect of Void-Generated Thermocapillary Convection on Dopant Segregation in Microgravity Solidification Experiments*, AIAA 2000-0703, Reno (2000).
5. J. A. Dean, *Lange's Handbook of Chemistry* (McGraw-Hill, New York, 1985).
6. J. Jasper, *J. Phys. Chem. Ref. Data* **1**:841 (1972).
7. P. Walden, *J. Phys. Chem.* **75**:555 (1911).
8. L. B. Gilman, 84th American Oil Chemists' Society Annual Meeting and Expo, Anaheim, CA, Apr. 27 (1993).
9. S. Hård, Y. Hamnerius, and O. Nilsson, *J. Appl. Phys.* **47**:2433 (1976).
10. P. Tin, J. A. Mann, W. V. Meyer, and T. W. Taylor, *Appl. Phys.* **36**:7601 (1997).
11. R. H. Katyl and U. Ingaard, *Phys. Rev. Lett.* **19**:64 (1967).
12. R. H. Katyl and U. Ingaard, *Phys. Rev. Lett.* **20**:248 (1968).
13. D. Langevin, *Light Scattering by Liquid Surfaces and Complementary Techniques*, Vol. 41, Surface Science Series (Marcel Dekker, New York, 1992).
14. R. V. Edwards, R. S. Sirohi, J. A. Mann, L. B. Shih, and L. Lading, *Appl. Opt.* **21**:3555 (1982).
15. L. Lading, J. A. Mann, Jr., and R. V. Edwards, *J. Opt. Soc. Am.* **A6**:1692 (1989).
16. E. Mazur and S. Chung, *Physica* **147A**:387 (1987).
17. K. Sakai, P.-K. Choi, H. Tanaka, and K. Takagi, *Rev. Sci. Instrum.* **62**:1192 (1991).
18. T. M. Jorgensen, *Meas. Sci. Technol.* **3**:588 (1992).
19. M. J. Timmerman and M. Hennaut-Roland, *J. Chim. Phys.* **27**:401 (1930).
20. M. J. Timmerman and M. Hennaut-Roland, *J. Chim. Phys.* **34**:693 (1937).
21. *Beilsteins Handbook of Organic Chemistry*, Database available electronically through DIALOG, File No. 390.